ISSN 1845–8319

THE EXPANSION AND RADIAL SPEEDS OF CORONAL MASS EJECTIONS

N. Gopalswamy[1], A. Dal Lago[2], S. Yashiro[3] and S. Akiyama[4]

[1] *Goddard Space Flight Center, Greenbelt, MD 20771, USA*
[2] *INPE, Sao Jose dos Campos, Brazil*
[3] *Interferometrics, Herndon, VA, USA*
[4] *The Catholic University of America, Washington DC, USA*

Abstract.

We show the relation between radial (V_{rad}) and expansion (V_{exp}) speeds of coronal mass ejections (CMEs) depends on the CME width. As CME width increases, V_{rad}/V_{exp} decreases from a value >1 to <1. For widths approaching 180°, the ratio approaches 0 if the cone has a flat base, while it approaches 0.5 if the base has a bulge (ice cream cone). The speed difference between the limb and disk halos and the spherical expansion of superfast CMEs can be explained by the width dependence.

Key words: coronal mass ejections - cone models - travel time

1. Introduction

For each CME, two speeds can be measured in the sky plane: the leading-edge speed (V_{LE}) at the position angle of the fastest moving front and the expansion speed (V_{exp}) defined as the rate at which the lateral dimension of a CME at its widest part increases with time (Dal Lago et al., 2003; Schwenn et al., 2005). Both V_{LE} and V_{exp} need to be converted to radial speeds (V_{rad}) to obtain the CME/shock travel time to Earth (see, e.g., Gopalswamy et al. 2001a). V_{LE} can be corrected to obtain the space speed assuming that the CME is a cone with a constant cone angle (Michalek et al., 2006; Xie et al., 2004; Zhao, 2008). For limb CMEs, one can determine the empirical relation between V_{exp} and V_{rad}, which can then be used for non-limb CMEs. The CME width is an output parameter of the cone models, whereas it is not considered in the empirical relationship (Dal Lago et al. 2003).

CMEs occurring close to the solar limb are not subject to projection effects, so the measured width is expected to be the true width. For a set

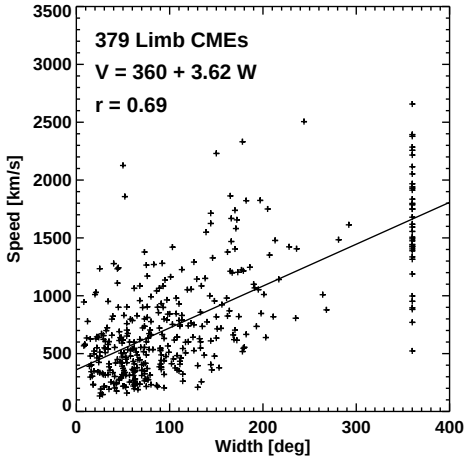

Figure 1: Scatter plot between the speed and width of limb CMEs, for which the central meridian distance (CMD) is large: $60^\circ \leq$ CMD $\leq 90^\circ$. CME width often increases with time early in the event and then becomes approximately constant, which we take as the width of a CME (see Yashiro et al., 2004 for details). The width ranges from about 10° to 360°. Data points vertically arranged at W = 360° correspond to halo CMEs (Howard et al., 1982).

of 22 limb CMEs that produced type II radio bursts (shock-driving CMEs), Gopalswamy et al. (2001b) found that the CME width (W) is linearly related to V_{LE}, with a correlation coefficient of 0.56. For a larger set of 379 limb CMEs (originating within 30° from the limb)shown in Fig. 1, one gets $V_{LE} = 360 + 3.62W$, where V_{LE} is in km/s and W is in degrees; the correlation coefficient is also better(0.69). The large scattering in Fig. 1 is likely to be due to different diffuse structures in different CMEs (Gopalswamy et al., 2008; Michalek et al., 2008) as well as the orientation of the neutral line with respect to the limb. If the neutral line is parallel to the limb, one expects to see a larger width than when it is perpendicular to the limb (Cremades et al., 2006). The mass (M) of a CME also depends on its width: $\log M = 12.6 + 1.3 \log W$, where M is in grams (Gopalswamy et al. 2005a). Thus the CME kinetic energy is heavily dependent on the CME width. The purpose of this paper is to show that the CME width affects the $V_{rad} - V_{exp}$ relation, which has implications for the CME travel time to Earth.

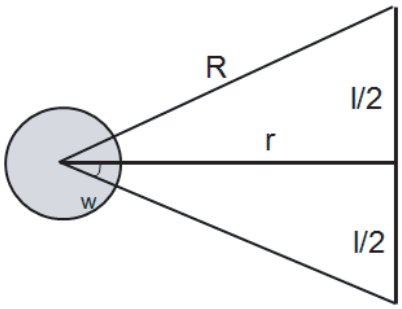

Figure 2: A CME cone defined for a CME originating from the limb. w is the cone angle, which is half the width of the CME ($W = 2w$). R is the edge length and r is the radial distance of the CME leading edge.

2. The CME Cone Models

We assume that a CME (originating at the limb) can be approximated by a cone, with its base representing the CME leading edge (see Fig. 2). The base of the cone is assumed to be circular, with a diameter l. The apex of the cone subtends an angle $2w$ at the center of the Sun. The height of the cone (r) represents the heliocentric distance of the CME leading edge. The distance to the leading edge along the sides of the cone is denoted by R. The cone defined in Fig. 2 is the flat cone as opposed to cones with a bulge at its base (which we refer to as ice cream cone). From the geometry of Fig. 2, we can write, $\tan w = (1/2)l/r$, which upon differentiation, gives,

$$dr/dt = (1/2)(dl/dt)\ \cot w \qquad (1),$$

where w is a constant for a given CME. Noting that $V_{exp} = dl/dt$ and $V_{LE} = dr/dt$ and that $V_{LE} = V_{rad}$ for limb CMEs, we get,

$$V_{rad} = f(w)V_{exp} \text{ with } f(w) = (1/2)\cot w \qquad (2).$$

Since w can vary from CME to CME, V_{rad} can be less than, equal to, or greater than V_{exp}. The empirical relation of Dal Lago et al. (2003), viz,

$$V_{rad} = 0.88V_{exp} \qquad (3)$$

becomes a special case of eq. (2) when $(1/2)\cot w = 0.88$ or $w = 29°.6$.

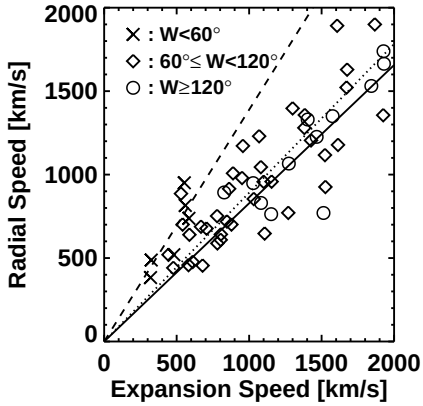

Figure 3: Scatter plot between the expansion and radial speeds for three width ranges: low(W<60°), intermediate (60° ≤W<120°), and large (W≥120°). Schwenn et al. (2005) had included CMEs narrower than 80° in the low-width group instead of the 60° used here. The regression lines in the low (dashed), medium (dotted), and large (solid) width groups are shown, whose slopes are 1.4, 0.89. and 0.83, respectively.

For CMEs wider than ∼60°, eq. (2) shows that $f(w)$ can be <0.88. For example, when $w = 45°$, eq. (2) gives $V_{rad} = 0.5V_{exp}$. On the other hand, for $w = 22°.5$, one gets $V_{rad} = 1.2V_{exp}$. For w approaching 90° or 0° the flat cone is no longer defined. For $w = 26°.56$, $V_{rad} = V_{exp}$.

The empirical relation (3) was obtained using the V_{rad} and V_{exp} values measured for a set of 57 limb CMEs (Fig. 3). When the CMEs are grouped into three width ranges, we find that the low-width CMEs (W <60°) have a different regression line compared to the higher-width ones. For CMEs with W <60°, V_{rad}/V_{exp} ∼1.4, which is substantially different from 0.89 (60° ≤W<120°) and 0.83 (W≥120°) for the higher-width CMEs, suggesting a clear width dependence. In terms of $f(w)$, the empirical relation (3) corresponds to $w = 29°.6$. All the data points lie between the lines corresponding to $w = 16°$ and 45°. Clearly, the regression line poorly represents the low-width CMEs and using it amounts to assuming that most of the CMEs have a width of 60°.

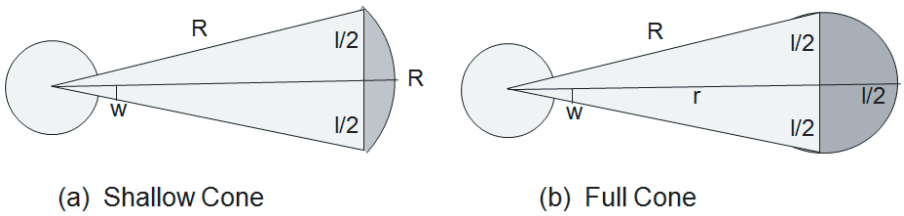

Figure 4: Modification of the flat cone in Fig. 2 resulting in a shallow ice cream cone (SIC, left) and a full ice cream cone (FIC, right). The symbols have the same meaning as in Fig. 2.

2.1. Ice cream Cone Models

From white light observations, one can infer that the CME leading edge is often curved with a concave outward shape. This means the flat-cone model described in Fig. 2 needs to be modified to account for such a curved-front shape (see, e.g., Schwenn et al., 2005). We approximate the CME shape by a shallow ice cream cone (SIC, Fig. 4a) and a full ice cream cone (FIC, Fig. 4b). For the SIC model, the radial extent R, at the edges of the cone and at the center are the same (see Fig. 4a), so $V_{rad} = dR/dt$. From the geometry in Fig. 4a, we get $\sin w = (1/2)(l/R)$, which can be differentiated to get $dR/dt = (1/2)(dl/dt)\,\mathrm{cosec}\,w$, or

$$V_{rad} = (1/2)\,\mathrm{cosec}\,w\;V_{exp} \qquad (4).$$

Equation(4) shows that $f(w)$ linking V_{rad} and V_{exp} ($f(w)$) has now a different form, but V_{rad} can be less than, equal to or greater than V_{exp} for different values of w. For example, $V_{rad} = V_{exp}$ happens when $w = 30°$. The empirical relation (3) is satisfied for $w = 34°.6$. Recall that eq. (2) implied $V_{rad} = V_{exp}$ for a smaller cone angle ($26°.56$).

FIC in Fig. 4b is the same as the flat cone as in Fig. 2, but a solid hemisphere of radius $l/2$ is attached to the base. In this case, $V_{rad} = d(r + l/2)/dt$. From the geometry of Fig. 4b, we can substitute $r = (1/2)\cot w$, so that $V_{rad} = (1/2)(1 + \cot w)(dl/dt)$ or

$$V_{rad} = (1/2)(1 + \cot w)V_{exp} \qquad (5).$$

Equation (5) shows yet another w-dependence of the V_{rad} - V_{exp} relation with higher values of w required for satisfying $V_{rad} = 0.88V_{exp}$ ($w = 52°.8$)

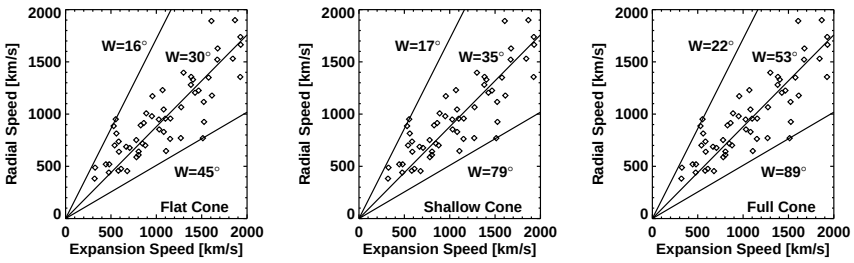

Figure 5: V_{rad} - V_{exp} scatter plots with the lines $V_{rad} = f(w)V_{exp}$ superposed for the flat cone (left), SIC (middle) and FIC (right). The w values corresponding to each of the lines are shown on the plots. All the data points lie between the upper and lower lines in each plot. The center line is the regression line (eq. 4) for the data points. Note that the average CME width at which the empirical relation is valid depends on the cone type (flat, SIC or FIC).

and for $V_{rad} = V_{exp}$ ($w = 45°$). For all cone models, V_{rad} dominates V_{exp} for narrow CMEs, while the reverse is true for wide CMEs. The critical width for $V_{rad} = V_{exp}$ depends on the leading edge shape (flat cone, SIC, or FIC). We considered these three examples because we can obtain simple analytic expressions for the V_{rad} - V_{exp} relationship. There may be intermediate situations.

Figure 5 compares the width ranges that bracket the data points in the scatter plot for the three cone models (flat, SIC and FIC). All the data points are contained within the two outer lines, which pass through the outermost point and the origin. The central line is the empirical relation (3), which depends on the cone type.

Figure 6 compares the relation $V_{rad} = f(w)V_{exp}$, where $f(w)$ is given by eqs. (2), (4), and (5) for the three cone models used. We see that for low widths, all the three models indicate $V_{rad} > V_{exp}$. When the width increases, the $f(w)$ of the three cone models separate, being the highest for the FIC model and the lowest for the flat cone model. As one approaches $w = 90°$, the flat cone is no longer defined. $f(w)$ approaches 0.5 for the SIC and FIC models. In other words, the expansion speed becomes twice the radial speed for the wide CMEs. Note that $f(w) = 0.88$ is a poor approximation for $f(w)$ over the range of observed CME widths.

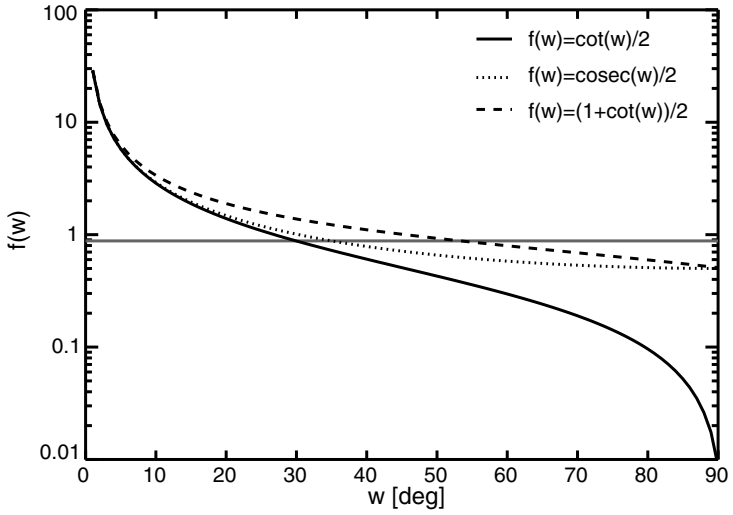

Figure 6: The function $f(w)$ that connects V_{rad} and V_{exp} for the three types of cones. The thin horizontal line at $f = 0.88$ represents the empirical relation (3).

3. Application to Halo CMEs

For an energetic CME erupting close to the disk center, we normally observe a symmetric full halo CME (Gopalswamy, 2004). For such a halo, the leading edge speed is half of the expansion speed. By observing the same CME from two orthogonal view points (such as by the STEREO mission), one can actually find the relation between V_{exp} and V_{rad}. For a coronagraph on the Sun-Earth line, one has to wait until the active region rotates from the disk center to the limb to get two orthogonal views (but not for the same CME). If we denote the leading-edge speeds of halo CMEs from the limb and disk as V_{limb} and V_{disk}, we see that $V_{limb} = V_{rad}$, and $V_{disk} = (1/2)V_{exp}$. From the average values of V_{limb} and V_{disk} (Gopalswamy et al., 2007), we see that $V_{rad} = 1533$ km/s and $V_{exp} = 1866$ km/s. This means $V_{rad}/\ V_{exp} = 0.82$, close to the empirical relation (3). Since halo CMEs are very energetic (average speed ∼1000 km/s), we infer from Fig. 1 that they must also be very wide. Using the average speed of ∼1000 km/s, we can infer an average width of ∼180° for the halo CMEs (cone angle ∼90°). Note that

for full halos, what is measured may be the shock around the CME (Sheeley et al., 2000), so the CME width may be overestimated. Nevertheless, we can conclude that halo CMEs correspond to the widest of the CMEs. When the solar activity picks up in cycle 24, coronagraphs on board the STEREO mission will observe the same CME from two viewpoints so we can verify the V_{rad} - V_{exp} relationship.

4. Application to Shock Travel Time

Schwenn et al. (2005) used eq.(3) to obtain a simple expression for the shock travel time (T) to 1 AU: $T = 203.0 - 20.77 \ln V_{exp}$. For symmetric full halo CMEs, $V_{exp} = 2V_{disk}$, so we can rewrite,

$$T = 188.6 - 20.77 \ln V_{disk} \qquad (6).$$

We test this relation for three well known symmetric full halos that resulted in huge geomagnetic storms: the Bastille Day event (2000 July 14), and the two Halloween 2003 CMEs (October 28 and 29). The sky-plane speeds (V_{disk}) of the three CMEs are 1674, 2459, and 2029 km/s (see Gopalswamy et al., 2005b), which when used in eq. (6) yield T = 34.4, 26.4, and 30.4 h, respectively. On the other hand, the observed shock transit times for these events are 27.9, 18.9, and 19.7 h, respectively (Gopalswamy et al., 2005b). Thus eq. (6) seems to significantly overestimate the travel times by 23%, 40%, and 54%, respectively for the three events. Since $V_{exp} = 2V_{disk}$, we get V_{exp} as 3348, 4888, and 4058 km/s, which when substituted in eq. (3), give the radial speeds as 2946, 4301, and 3571 km/s. If we use these radial speeds into the empirical shock arrival model (see Gopalswamy et al., 2005b,c), viz.,

$$T = ab^V + c$$

with

$$a = 151.002; b = 0.998625; c = 11.5981 \qquad (7),$$

we get the travel times as 14.2, 12.0, and 12.7 h, respectively. These values are substantially below the observed T. When the Xie et al., (2004) cone model (similar to the flat cone) is used, the radial speeds are substantially lower: 1741, 2754, and 2049 km/s (see Gopalswamy et al., 2005d), which when used in eq. (7), give travel times as 25.9, 15.0, and 20.6 h, much closer to the observed T. Interestingly, when the observed V_{disk} are used in (7),

we get T as 26.7, 16.7, and 20.9 h, which are similar to, if not better than, the T values obtained from cone-model radial speeds. In fact, the ratios of the cone-model radial speed to the expansion speed become 0.52, 0.56, and 0.50, suggesting $V_{rad} = (1/2)V_{exp}$. Such a relation applies to CMEs with the highest width as illustrated in Fig. 6. This relation also tells us that the radial speed is roughly same as the sky-plane speed (V_{disk}) because $V_{disk} = 0.5V_{exp}$ by definition. $V_{disk} = V_{rad}$ implies that such CMEs expand spherically above the solar surface. Therefore, the empirical relation (3) is not applicable to extreme events.

5. Summary and Conclusions

From a simple geometrical analysis, we have shown that the V_{rad} - V_{exp} relationship depends on the width of the CMEs and the amount of material in the CME leading edge. The observed scatter in the V_{exp} and V_{rad} plots can therefore be accounted for by the variation of CME width from event to event. We also found that the empirical relationship between V_{rad} and V_{exp} (Dal Lago et al., 2003) is generally valid for "average" CMEs, but it can be substantially different for the narrow and very wide CMEs. The difference in average speeds of limb and disk halo CMEs suggests a relationship $V_{rad} = 0.82V_{exp}$, very similar to the empirical relationship. However, for very wide CMEs, the relationship becomes $V_{rad} = 0.5V_{exp}$, which we demonstrated using some well known symmetric full halo CMEs. The radial speed obtained from a CME cone model and the observed leading edge speed in the sky plane were found to be substantially similar for superfast full halo CMEs, implying spherical expansion in such extreme cases.

Acknowledgements

We thank G. Michalek for help in manuscript preparation. Work supported by NASA's LWS TRT program.

References

Cremades, H., Bothmer, V., Tripathi, D.: 2006, *Adv. Space Res.*, **38**, 461.

Dal Lago, A., Schwenn, R., and Gonzalez, W. D.: 2003, *AdSR* **32**, 2637.

Gopalswamy, N.: 2004, *A global picture of CMEs in the inner heliosphere, in The Sun and the Heliosphere as an Integrated System, edited by G. Poletto and S. T. Suess, Kluwer Acad., Boston.*, 201.

Gopalswamy, N. Lara, A., Yashiro, S., Kaiser, M. L., Howard, R. A.: 2001a, *J. Geophys. Res.*, **106**, 29207.

Gopalswamy, N. Yashiro, S., Kaiser, M. L., Howard, R.A., Bougeret, J.-L.: 2001b, *J. Geophys. Res.* **106**, 29219.

Gopalswamy, N., Aguilar-Rodriguez, E., Yashiro, S., Nunes, S., Kaiser, M. L., Howard, R. A.: 2005a, *J. Geophys. Res.* **110**, A12S07.

Gopalswamy, N., Yashiro, S., Liu, Y., Michalek, G., Vourlidas, A., Kaiser, M. L., Howard R. A.: 2005b, *J. Geophys. Res.* **110**, A09S15.

Gopalswamy,N. Lara, A., Manoharan, P. K., Howard, R. A.:2005c, *Adv. Space Res.*, **36**, 2289.

Gopalswamy N., Xie H., Yashiro S., Usoskin I.: 2005d, *Proc. 29th International Cosmic Ray Conference, Pune*, **1**, 169.

Gopalswamy, N., Yashiro, S., Akiyama, S.: 2007 *J. Geophysical Res.*, **112**, A06112.

Gopalswamy, N., Yashiro, S., Xie, H., Akiyama, S., Aguilar-Rodriguez, E., Kaiser, M. L., Howard, R. A., Bougeret, J.-L.: 2008, *Astrophys. J.* **674**, 560.

Howard, R. A., Michels, D.J., N. R. Sheeley N.R., Jr., M. J. Koomen, M. J.: 1982, *Astrophys. J.*, **263**, L101.

Michalek, G., Gopalswamy, N., Lara, A., Yashiro, S: 2006, *Space Weather*, **4**,S10003.

Michalek, G., Gopalswamy, N., Yashiro, S.: 2008, *Solar Phys.*, **248**, 113.

Schwenn, R., Dal Lago, A., Huttunen, E., Gonzalez, W. D.: 2005 *Annales Geophysicae* **23**, 1033.

Sheeley, N. R., Jr., Hakala, W. N., and Wang, Y.-M.: 2000, *J. Geophys. Res.* **105**, 5081.

Xie, H., Ofman, L., Lawrence, G.: 2004, *J. Geophys. Res.* **109**, 3109.

Yashiro, S., Gopalswamy, N., Michalek, G., St. Cyr, O. C., Plunkett, S. P., Rich, N. B., Howard, R. A.: 2004, *J. Geophys. Res.* **109**, 7105.

Zhao, X.-P.: 2008, *J. Geophys. Res.* **113**, A02101.